Arabian Journal for Science and Engineering
https://doi.org/10.1007/s13369-024-09063-w

RESEARCH ARTICLE-CIVIL ENGINEERING

A Simulation-Based Investigation on Thermal Responses of Suspension Bridge Tower Under Different Fire Scenarios

Sara Mostofi[1] · Ahmet Can Altunişik[1,2,3] · Yunus Emrahan Akbulut[1] · Fatih Yesevi Okur[1]

Received: 7 July 2023 / Accepted: 3 April 2024
© The Author(s) 2024

Abstract
Records of bridge fire incidents illustrate that bridge fires can have catastrophic consequences. The severity of these fires can be influenced by various factors such as bridge type, vehicle size, and wind. Contrary to building fires that have been extensively studied, scant attention has been paid to bridge fires and more specifically fire exposure to the suspension bridges. In addition, existing bridge fire literature is mostly concentrated on fire exposure to girders or cables of suspension bridges. Therefore, this study focused on the post-fire condition of a fire-exposed suspension bridge tower using computational fluid dynamics (CFD) modeling techniques and finite element analysis (FEA). The impacts of the main bridge fire parameters including vehicle size, exposure duration, distance between the fire source and tower, and wind effects were also evaluated. Initially, fire dynamic simulator (FDS) was used to simulate 12 different fire scenarios. The time–temperature histories obtained from each scenario were transferred to the ABAQUS finite element (FE) software to conduct transient thermal analysis and obtain the temperature development within the steel tower of the bridge. The post-fire evaluation was performed with respect to the temperature-induced reduction in the yield strength of steel. The results show that fire exposure from a fuel truck in the proximity of a steel tower could significantly reduce the strength of the tower and lead to severe damage. Early control of the fuel truck fire is crucial in reducing the severity of the damage and preventing temperature development in higher areas of the tower. Although a wind toward the tower can significantly increase the fire-induced damage to the bottom parts of the tower, it considerably reduces the temperature exposure to the higher parts of the tower. Fire exposure from a normal vehicle does not put the tower at risk of failure, and an unprotected steel tower can withstand it. However, a bus fire may lead to minor damage. The thermal strengthening of the first 20 m of the tower can help in preventing the potential fire damage.

Keywords Bridge fire · Finite element analysis · Suspension bridge · Steel tower · Thermal analysis

1 Introduction

Fire poses a significant threat to structures, with serious consequences. The recent surge in urbanization has escalated transportation demands, thereby increasing the incidence of bridge fires. Such damage disrupts local transportation, causing cascading effects on connected networks [1, 2]. Exposure of bridges to fire can inflict severe damage, resulting in substantial direct and indirect economic losses [2–4]. Studies by Garlock et al. [5] and Peris-Sayol et al. [6] have thoroughly evaluated bridge fire incidents, highlighting some of the most significant events, including the catastrophic MacArthur Maze fire in Oakland, which caused partial collapse and major economic losses [7–10]. These incidents underscore the critical need for bridge fire evaluation and safety measures. However, considering fire load for all bridges is economically unfeasible. Thus, identifying fire-vulnerable bridges and incorporating fire considerations in their design and post-construction assessment is essential [11–13].

Bridge fires are commonly initiated by the collision or overturning of vehicles carrying gasoline-based fuels [14]. Gasoline, with its very low flash point, can ignite instantly,

✉ Ahmet Can Altunişik
ahmetcan@ktu.edu.tr; ahmetcan8284@hotmail.com

1 Department of Civil Engineering, Karadeniz Technical University, Trabzon, Turkey

2 Earthquake and Structural Health Monitoring Research Center, Karadeniz Technical University, Trabzon, Turkey

3 Dynamic Academy Software, Construction Ind. Trade. Co. Ltd., Trabzon, Turkey

Published online: 28 May 2024

burning at a high heat release rate (HRR), rapidly spreading over the spilled area, and reaching high temperatures in the initial stage of the fire [6–8]. This immediate and intense exposure to fire poses a critical threat to bridge structures, particularly those constructed of steel. The inherent sensitivity of steel to high temperatures makes these structures prone to fire damage and collapse [3, 5, 6]. Such susceptibility is due to the temperature-dependent material properties of steel, which, when exposed to fire, experience rapid temperature increases and significant reductions in yield strength and stiffness. These reductions compromise the structural integrity and load-bearing capacity of steel elements [14–17]. This highlights the importance of comprehensive fire evaluations to assess and mitigate the considerable risks associated with fire exposure to unprotected steel elements of bridges.

Despite the devastating outcomes of previous bridge fires, current bridge design guides and standards largely overlook fire resistance [2, 8, 18]. The NFPA 502 standards address fire loads in long bridges [19] but lack detailed specifications for fire loading considerations or guidelines for post-fire assessments [20]. This gap points out the critical need for continued research and development. Consequently, bridge fire remains a challenging subject for structural fire engineers, prompting several studies to investigate the fire behavior of bridges through experimental research [21–25]. Among these, Vimonsatit et al. analyzed the shear capacity degradation in steel girders under controlled high temperatures and suggested that traditional steady-state fire conditions employed in tests might not encompass the complexities of actual fire scenarios [26]. Complementarily, the dual experimental and finite element analysis approach by Aziz et al. has emphasized the vulnerability of steel girder bridges to standard fire exposure, indicating potential structural failure within 30 min [27]. Alos-Moya et al. further expanded this knowledge by conducting full-scale fire tests and revealed the significant influence of fire position and fuel quantity on bridge performance [25]. Beneberu et al. have argued that standard fire curves do not realistically simulate the bridge fire conditions and emphasized the role of environmental factors such as wind [24]. Experimental studies by Chen et al. and Zhang et al. delved into the thermal response of steel cables and wires [23, 28]. Chen et al. observed that factors such as wind and fire source location are critical, and Zhang et al. found that exposure to temperatures above 500 °C significantly reduces the static and fatigue strength of steel wires which is a critical component of suspension bridges. Song et al. evaluated the failure mechanisms of steel–concrete composite bridge girders under fire. They observed that all tested girders suffered severe deflection leading to failure, especially in open-section designs [22]. These findings point to the need for detailed assessments of bridge components under fire conditions, while including the influences of environmental conditions and structural geometry.

Although experimental studies provide essential data, they are often expensive and complex, particularly when it comes to full-scale fire tests. The progression in numerical modeling, however, has significantly enriched the understanding of bridge behavior under fire. Bennetts and Moinuddin developed a numerical model to assess the fire vulnerability of cable-stayed bridges, particularly highlighting the risk to unprotected steel cables under extreme fire conditions [29]. The advanced ABAQUS modeling conducted by Payá-Zaforteza and Garlock revealed that real fires might cause longer failure times than those predicted based on standard curves, especially in carbon steel bridges [30]. Alos-Moya et al. used FDS and ABAQUS to replicate a real fire event and observed that standard building fire curves might overestimate structural endurance, while hydrocarbon curves could offer a less conservative estimation [10]. Gong et al. emphasized the critical impact of fire duration, intensity, and position on the vulnerability of cable-supported bridges [31]. Peris-Sayol et al. found fire position and wind speed to be crucial in steel bridge vulnerability, using FDS and ABAQUS for analysis [32]. Alos-Moya et al. have used experimental data to fine-tune the numerical models for bridge fires and confirmed the precision of FDS simulations for gas temperature estimation [33]. Cui et al. employed FDS and ANSYS to investigate the fire stability issues in a three-pylon suspension bridge and emphasized the importance of rapid fire suppression for preserving the stability of suspension bridges [34]. Zou et al. noted the significant role of wind on bridge hangers, with wind playing a substantial role in temperature rises [35].

Building on previous studies that emphasized the importance of fire evaluations for bridges, this study contributes further by analyzing the fire behavior of suspension bridge towers, critical for load bearing, and maintaining overall stability of these bridges [36]. The objective of this research is to determine the impact of fire on steel towers of suspension bridges and analyze the effects of fire on these steel towers, focusing on the role of size, distance, exposure time, and wind in their fire response. This methodology aims to identify and analyze key factors that affect the fire response of suspension bridge towers and to evaluate the implications of these factors on the yield strength of fire-exposed tower, ultimately determining its post-fire condition.

To conduct the fire evaluations, the iconic Bosphorus suspension bridge was chosen, focusing on exposure of one tower to a vehicle fire. The study initiated with simulating fire conditions across various scenarios to understand the fire behavior and obtain realistic time–temperature records. The gathered temperature records were then used in ABAQUS finite element (FE) software [37] for transient thermal analysis, enabling the assessment of temperature variations within

section of the tower. The analysis aimed to determine the strength reductions under each scenario, thereby assessing the post-fire condition of the tower.

2 Methodology

The performed bridge fire evaluation comprised three main phases: FDS simulations for twelve scenarios, ABAQUS thermal analysis for each, and subsequent post-fire evaluations. Pyrosim [38], a CFD simulation program, was used to model fire behavior under diverse conditions, including different vehicle types (passenger car, bus, fuel truck), exposure durations, distances (fire on lanes 1–3), and weather conditions (with and without wind). The selection of these parameters was based on past studies, indicating that the size of the fuel source, proximity to the bridge, and wind conditions significantly influence bridge fire responses. To accurately assess the impact of exposure duration and vehicle type, two conditions were examined: one based on variable burning durations from Ma et al.'s bridge fire study [39] where the burning duration varies in accordance with the fire size, and another assuming a uniform burning duration of 30 min for all vehicles. The fuel truck scenario, due to its larger dimensions, is identified as potentially the most destructive in terms of fire severity. Therefore, the impact of wind and distance was specifically analyzed for this vehicle type. The considered fire scenarios are outlined in Table 1. Following each simulation, the generated time–temperature curves were imported into ABAQUS for transient heat transfer analysis to determine the temperature distribution within the tower. The obtained temperatures were used to evaluate the strength reduction and assess the post-fire condition of the tower.

Scenarios FS6 and FS7 involve the same vehicle size and fire conditions but are designated with different scenario names (VS for FS6 and FD for FS7) to distinguish their use in analysis. FS6 focuses on comparing the vehicle size, while FS7 is used to assess the impact of distance on fire behavior. This differentiation ensures clarity in the presentation and discussion of results across various aspects of the study.

3 Case Study

The Bosphorus Bridge, spanning the Bosphorus Strait and linking the Asian and European sides of Istanbul (Fig. 1), has been a vital transportation hub since 1973. This bridge, which was designed by Sir Gilbert Roberts, William Brown, and Michael Parsons, has a main span of 1074 m, side spans of 255 m (Asian) and 231 m (European), totaling 1560 m in length with a 33.4-m deck accommodating 6 lanes over a 28-m clear road width. The towers are 165 m high constructed from hollow steel sections, supported with horizontal beams for enhanced lateral stability (Fig. 2). The bridge was designed to withstand a live load of 1.33 tons/m and wind speeds up to 45 m/s, supporting an average daily traffic of 3900 vehicles per hour [40]. After 40 years, it underwent a year-long maintenance in 2013, including the replacement of all hangers.

4 Fire Dynamic Simulation

To simulate fire scenarios, Pyrosim, a graphical interface for the fire dynamics simulator (FDS) developed by National Institute of Standards and Technology (NIST), was utilized. FDS, a Fortran-based CFD code, is utilized to model fire-driven flows, providing essential engineering data such as gas temperature and heat flux [42]. The modeling process in FDS involves constructing the basic model of the structure, defining the control volume and boundary conditions, selecting mesh size, creating the fire source, specifying material properties, characterizing the combustion model, and positioning measurement devices to capture necessary outputs.

To simulate the bridge fire scenarios, Pyrosim was used to develop a model representing the first 400 m of the bridge from the European side, focusing on the area around one tower due to its long span and localized fire exposure. The control volume was selected in a way that could encompass both the bridge elements and their immediate surroundings. Mesh size and control volume dimensions were determined from a mesh convergence study, ensuring finer meshing around the fire source and progressively coarser meshing with increasing distance. The airflow around the bridge was simulated by setting all sides of the control volume, except the bottom, to open boundaries.

After creating the bridge geometry and specifying boundary conditions, we defined the material properties: the bridge deck is made of concrete, while all other elements are constructed from steel, using the software's predefined material library. Concrete surfaces were categorized as solid surfaces with voids, and steel sections as exposed solid surfaces.

The intensity of a fire is characterized by its heat release rate (HRR), the energy release rate for each fire case [43]. Before creating the fire source, the HRR for each vehicle size was determined. Equation (1) is used to calculate the pool diameter and the HRR relevant to each scenario.

$$Q = \dot{m}'' \times \Delta H_c (1 - e^{-k\beta d}) \times A_{\text{fire}} \tag{1}$$

where Q (kW) is HRR of the fire, $k\beta$ (m^{-1}) is the empirical constant, $\dot{m}''$ ($\text{kg/m}^2\text{/s}$) is the mass burning rate, d is the diameter of pool fire (m), ΔH_c (MJ/kg) is the heat of combustion, and A_{fire} (m^2) denotes the spill area.

Table 1 Overview of the scenarios

Scenario name	Variable parameters	Vehicle type	Fire size (m)	Burning time (s)	Distance from tower (m)	Wind condition (m/s)
FS1	VS1/BT1	Passenger Car	1.5 × 4.0	2700	1.00	No wind
FS2	VS2/BT2	Bus	2.0 × 6.0	5400	1.00	No wind
FS3	VS3/BT3	Fuel truck	7.0 × 12.0	7200	1.00	No wind
FS4	VS1	Passenger car	1.5 × 4.0	1800	1.00	No wind
FS5	VS2	Bus	2.0 × 6.0	1800	1.00	No wind
FS6	VS3	Fuel truck	7.0 × 12.0	1800	1.00	No Wind
FS7	FD1	Fuel truck	7.0 × 12.0	1800	1.00	No wind
FS8	FD2	Fuel truck	7.0 × 12.0	1800	5.60	No wind
FS9	FD3	Fuel truck	7.0 × 12.0	1800	10.34	No wind
FS10	FD1/Wind	Fuel truck	7.0 × 12.0	1800	1.00	33.3
FS11	FD2/Wind	Fuel Truck	7.0 × 12.0	1800	5.60	33.3
FS12	FD3/Wind	Fuel truck	7.0 × 12.0	1800	10.34	33.3

**VS* Vehicle Size, *BT* Burning Time, and *FD* Fire Distance from the element



Fig. 1 Bosphorus suspension bridge [41]

The heat of combustion, mass burning rate, and empirical constant for gasoline were sourced from the SFPE Handbook of Fire Protection Engineering [44]. HRR values were input into the software as heat release rate per unit area (HRRPUA), and the fire source for each scenario was modeled using a rectangular burner on the deck, 60 m above sea level, with dimensions matching the spill area. Gasoline combustion parameters, along with HRR for each vehicle, are detailed in Table 2. Given the complex composition of Gasoline, its fire reaction was approximated to that of Octane, as recommended in the SFPE Handbook.

To capture the development of gas temperatures in each scenario, thermocouples were positioned at the sides and middle of the burner surface, spaced at vertical intervals of 1 m along the tower's height. Additionally, to monitor the instantaneous temperature exposure, adiabatic surface temperature (AST) recording devices were installed at every 1 m along the tower to monitor real-time temperature exposures, ensuring a detailed capture of the vertical temperature gradient. This high-resolution data collection approach, coupled with thermal analysis performed for each 1 m segment of the tower, aimed to precisely illustrate temperature changes along the tower's height. The simulation of 12 fire scenarios, conducted on a system with 24 cores and 2.4 GHz speed, required approximately 1176 h.

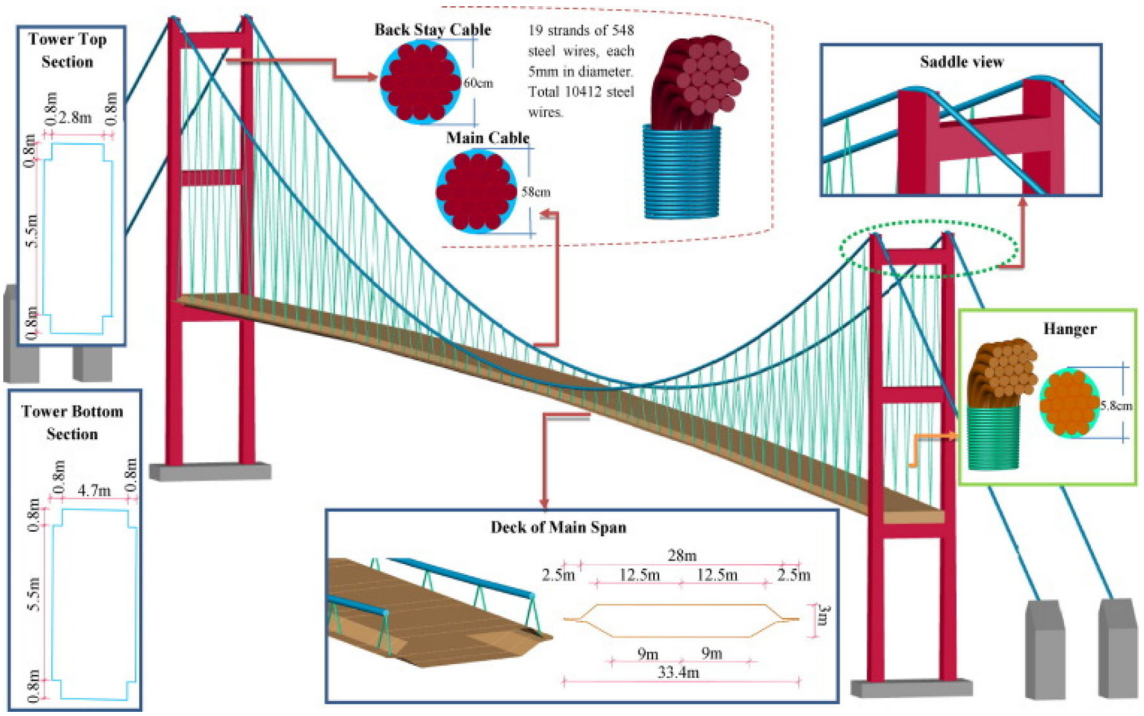

Fig. 2 Schematic overview of Bosphorus suspension bridge [41]

Table 2 Combustion parameters for each vehicle

Parameters	Passenger car	Bus	Fuel truck
m''(kg/m^2/s)	0.055	0.055	0.055
ΔH_c (MJ/kg)	4.37×10^4	4.37×10^4	4.37×10^4
$k\beta$ (m^{-1})	2.1	2.1	2.1
A_{fire} (m^2)	1.5×4.0	2.0×6.0	7.0×12.0
D (m)	2.764	3.909	10.342
HRR (kW)	14,377	28,834	201,894
α (kW/s^2)	0.011	0.123	1
Radiative Fraction	0.35	0.35	0.35
Soot yield	0.038	0.038	0.038
CO yield	0.011	0.011	0.011

5 Fire Simulation Results

The behaviors of fire and smoke, as well as the direction of heat movements derived from each scenario, are illustrated in Figs. 3 and 4. This research has defined damage criteria based on the steel elements reaching a pivotal temperature threshold of 600 °C, beyond which the likelihood of structural failure under service loads significantly increases [45–48]. In discussing the results, the fire location on the bridge deck, which is at 60 m, is considered the reference point, set at 0 m. Thus, when referring to locations above the deck, they are described relative to this base level (e.g., 5 m, 10 m above the deck), rather than their absolute height above sea level. Figure 6 presents the gas temperature data obtained from each scenario.

After 30 min of burning, the fuel truck exhibited a significantly higher flame and denser smoke cloud compared to the other vehicles. Its large spill area led to substantial smoke accumulation in front of the tower, whereas smoke from passenger car and bus fires was thinner and more dispersed. The significant flame height and smoke density observed in the fuel truck scenarios are attributable to its larger fuel load, resulting in a more intense heat release rate. The extensive spill area contributes to a denser accumulation of smoke, which could surround structural elements more substantially and sustain higher temperatures over time, leading to potential steel strength degradation at a faster rate.

Variations in burning duration point out the dynamic nature of fires. The extended burn time of 7200 s for the fuel truck notably increases both the flame height and smoke density, exacerbating thermal exposure and potential structural damage. This could be due to the sustained availability of fuel, maintaining a high heat release rate. The longer a fire burns, the more heat is imparted to the bridge structure, increasing the potential for damage. However, this is not a simple linear relationship. As the fire progresses, the rate of combustion can change as the available fuel is consumed as demonstrated the passenger car fire demonstrates a decrease in intensity after 2700 s, possibly due to the consumption of available fuel and a reduction in energy release. The bus, with

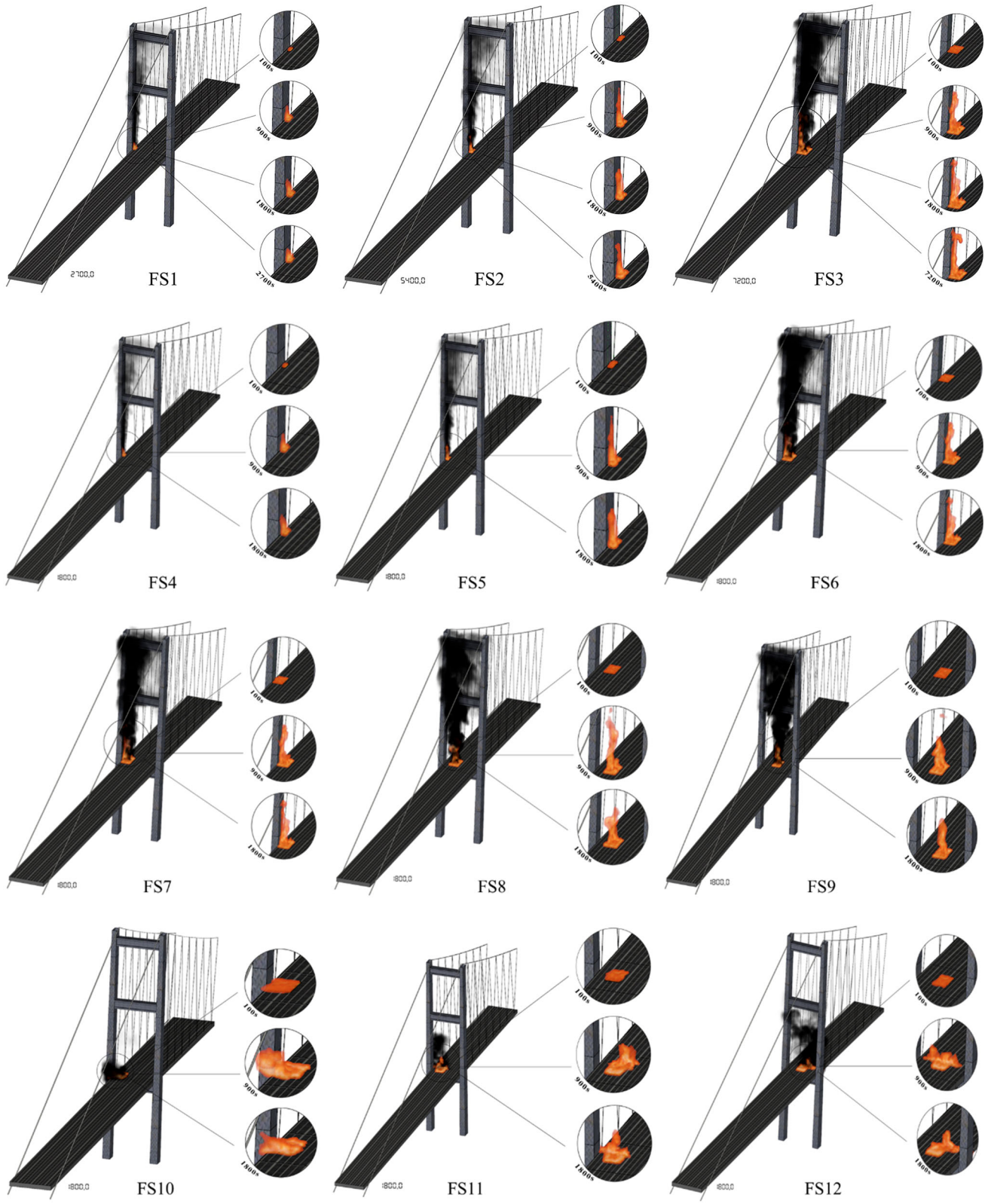

Fig. 3 Flame and smoke behavior in different scenarios

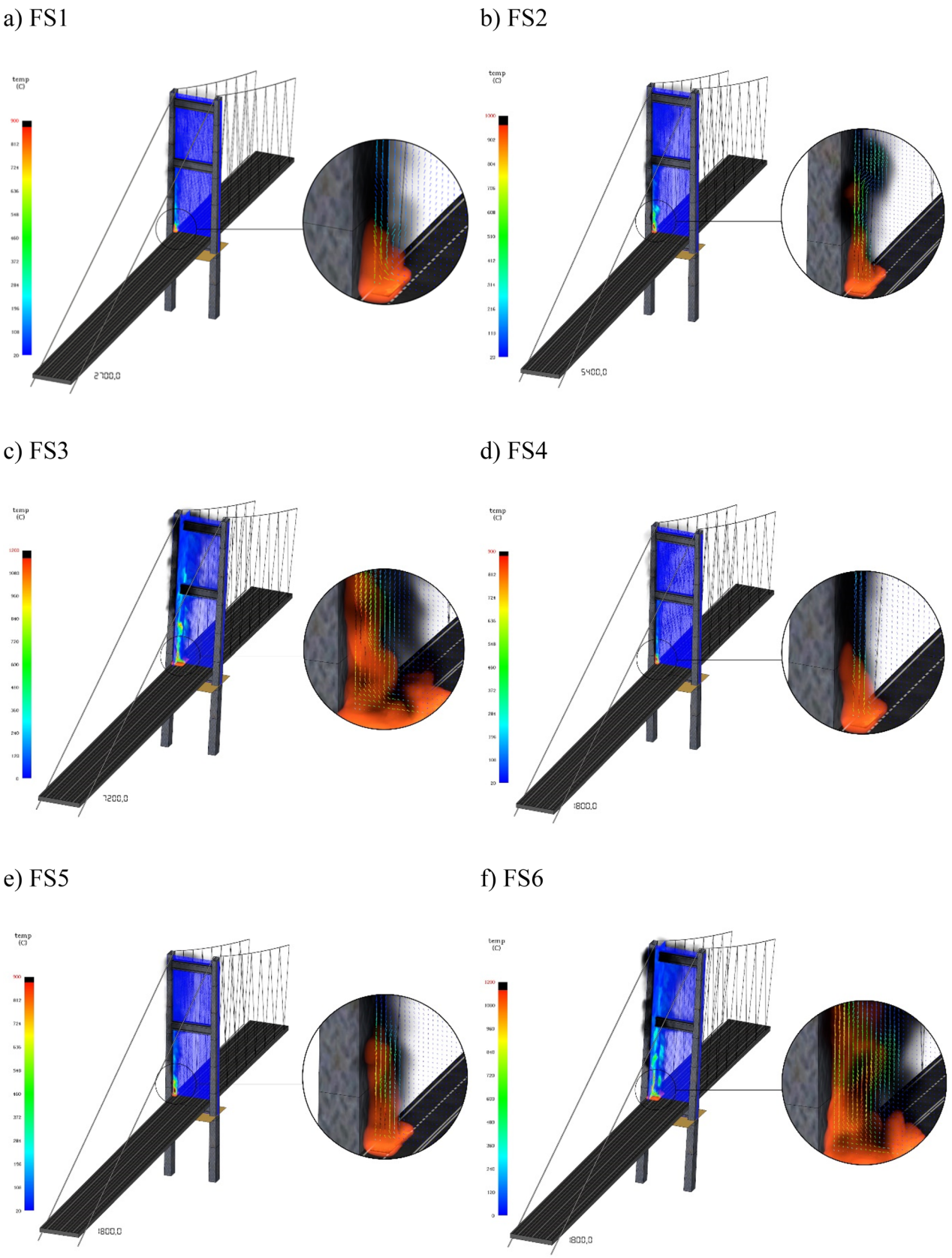

Fig. 4 Heat flow directions in each scenario

g) FS7

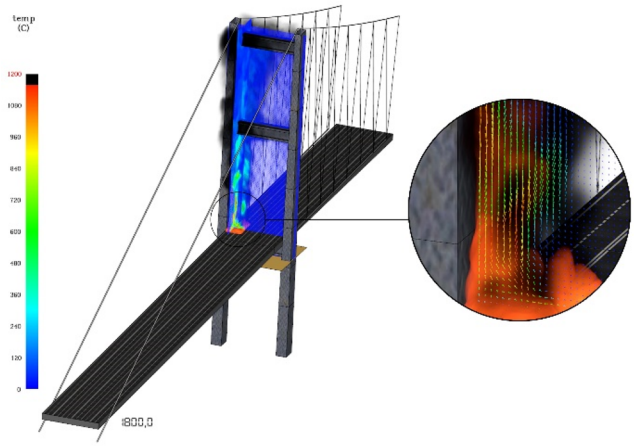

h) FS8

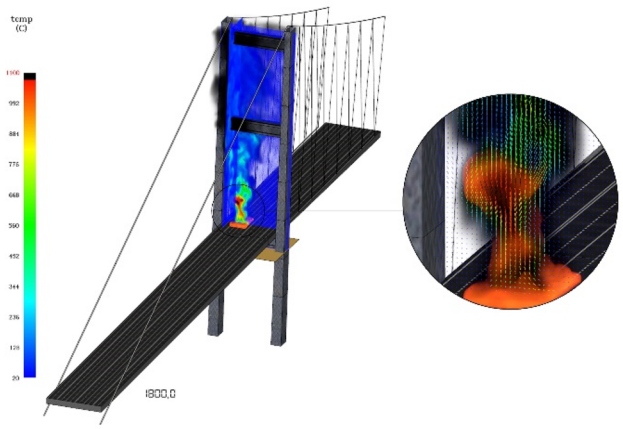

i) FS9

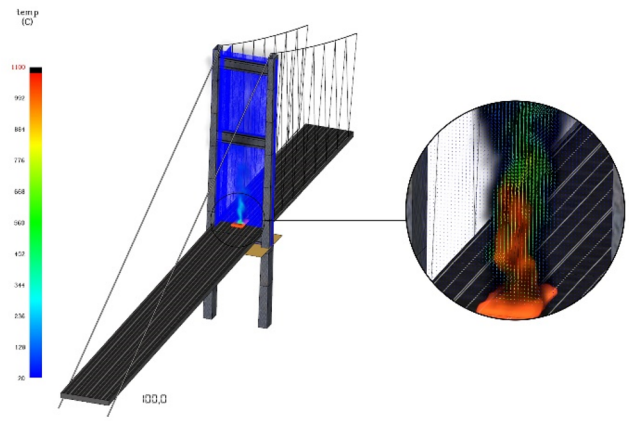

j) FS10

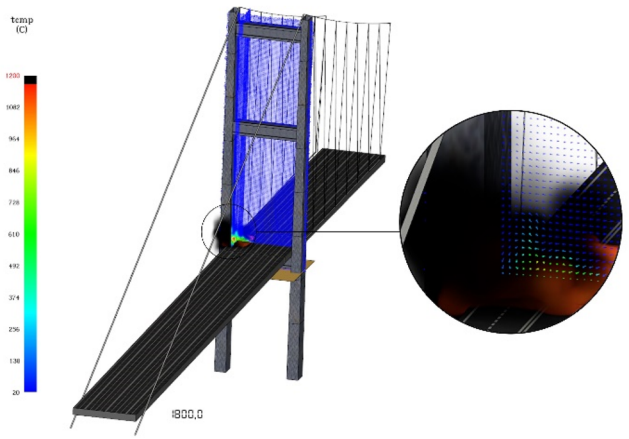

k) FS11

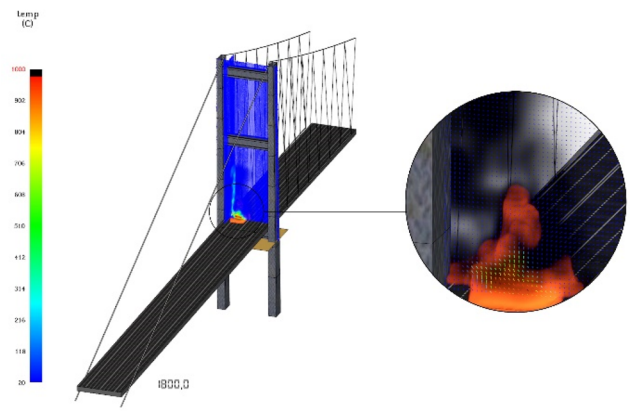

l) FS12

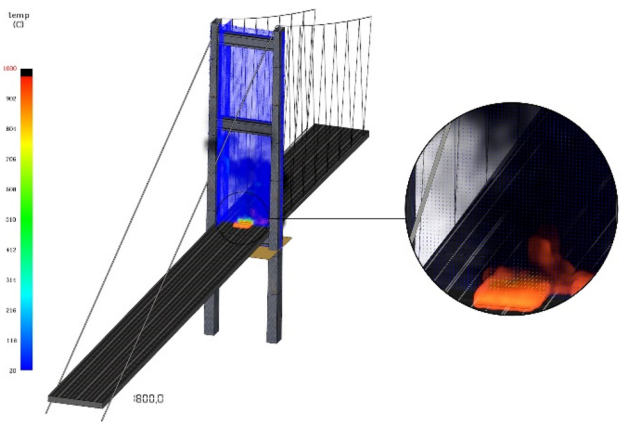

Fig. 4 continued

its intermediate fuel load, demonstrated only minor changes over the 5400 s duration, which shows the balance between fuel consumption and heat output.

The proximity of fires to the tower significantly influences the thermal load on the structure. The Coanda effect, evident in scenarios close to the tower, intensifies this impact by directing heat and flames along the surface of the tower, as depicted in Fig. 4, thereby increasing thermal exposures and risk of localized overheating. This phenomenon is particularly critical for fires in lanes closest to the tower, which can lead to uneven temperature distribution and potential localized structural failures. Conversely, fires situated in the second and third lanes generally produce an upward movement of heat, diminishing direct thermal exposure to the tower. Yet, this does not necessarily equate to a reduced risk, especially when considering the influence of wind, as demonstrated in scenarios FS10–FS12. Wind has been shown to decrease flame height and extend flame depth, and in certain scenarios, it causes flames to flicker toward the tower, enhancing localized heating at lower levels while potentially cooling higher sections. These findings underscore the importance of incorporating strategic fire barriers and fire-resistant materials in bridge design. The overall behavior of the flame and smoke is summarized in Table 3.

Figure 5 presents the temperature gradient at the base of the tower across different fire scenarios. Notably, FS10, characterized by the proximity of the fire to the tower coupled with y-direction wind, registers the highest base temperatures. The fuel truck fire, due to its extensive fuel reservoir, exhibits a base temperature that is 42% higher compared to passenger cars and buses, emphasizing the significant influence of vehicle type and fire size on the resultant thermal load. Although the duration of burning does not drastically alter the peak temperatures reached, it profoundly affects the tower by prolonging heat exposure. A more extended duration allows for a continued radiation of heat, which intensifies the fire load and potential damage to the tower. This is particularly evident within the first 20 m from the fire's origin, where thermal impact is concentrated.

Distance from the fire plays an influential role in the thermal gradient experienced by the tower. For instance, FS7, which involved a fire on the first lane, demonstrated a pronounced increase in the base temperature, fluctuating between 800 and 1100 °C. This significant elevation in temperature emphasizes the threat posed by fires that occur close to the tower, as the heat can easily reach levels that degrade the mechanical properties of steel and lead to potential failure. In scenarios with varying distances, the temperature predominantly affects the area within the first 25 m of the fire's vertical plane. However, when wind is introduced into the system, this area of influence narrows to below 15 m of the tower. Wind conditions not only impact the orientation of the flame, causing it to tilt toward the tower in the case of FS7, but also moderate flame temperatures in the scenarios with fires on the second and third lanes. Here, the wind effectively reduces the thermal load on the tower, as evidenced by the decreased temperatures observed in these scenarios.

6 Finite Element Modeling

After the fire simulation and obtaining AST time–temperature data, thermal analyses were conducted using ABAQUS. In this process, the obtained temperatures were applied as a thermal load to the bridge tower. This analysis aimed to determine the cross-sectional temperature distribution of the elements during the fire. Thermal analysis incorporated material properties including density, thermal conductivity, and specific heat. Consequently, the outcome of the heat transfer analysis provided transient nodal temperatures, which were calculated based on conduction, convection, and radiation heat transfer modes. The impact of fire on the tower, through radiation and convection, was assessed using the Robin boundary condition, as demonstrated in Eq. (2).

$$h_{net} = \alpha_c(\theta_g - \theta_m) + \varepsilon_m \varepsilon_f \sigma^{sb}\left[(\theta_g - 273)^4 - (\theta_m + 273)^4\right] \tag{2}$$

where h_{net} (W/m^2) denotes net heat flux, α_c (W/m^{2}K) is the convective heat transfer coefficient, θ_g and θ_m (°C) are represent the fire temperature and surface temperature of the structural member, respectively, ε_m and ε_f are the emissivity of the exposed surface and fire, respectively, and σ^{sb} is Stefan–Boltzmann constant, which is equal to 5.67×10^{-8} (W/m^{2}K^4).

The heat transfer analysis conducted included creating the geometry of the tower section, defining both temperature-dependent and non-temperature-dependent material properties, determining the appropriate meshing, and applying the temperature load.

6.1 FE Model Generation

Since only the tower will be involved in thermal analysis, it was not required to generate the FE model of the whole bridge and only the tower was modeled. To accurately capture the temperature distribution, it is important to have very small elements in a very fine mesh. But it can also significantly increase the computational cost for very large elements. Therefore, to have a balance between accuracy and computational time, a 2D FE model of the tower was generated. This simplification approach was previously adopted by different researchers [49, 50]. In the 2D model, the temperature distribution along the height direction will be ignored, and instead, in the fire simulation, the temperature was recorded at every 1 m from the tower's height.

Table 3 Summary of fire behavior in different scenarios

Vehicle type	Environmental condition			
	No wind		Windy	
	Flame	Smoke	Flame	Smoke
Passenger car	Relatively low—inclined toward tower	Light and scattered	N/A	N/A
Bus	Medium–low—inclined toward tower	Average density	N/A	N/A
Fuel truck 1st lane	Very high—inclined toward the tower	Densely covered the exposed surface of tower	Low height, flickering toward tower	Densely covered the bottom part of tower
Fuel truck 2nd lane	Very high—moving upwards	Very thick smoke cloud	Low height, scattering around spill area—more depth	Lower smoke concentration
Fuel truck 3rd lane	Very high—moving upwards	Very thick smoke cloud	Much lower height and higher depth—scattering around the spill area	Lower density, more horizontal boundaries

To start the heat transfer analysis, a 2D geometry of the tower with a cross-sectional dimension of 7.17 × 4.00 m and thickness of 0.02 m was developed in ABAQUS (Fig. 6). To model the tower geometry, the DC2D4 2D solid continuum element was employed. This element is 4-node linear and is suitable for conducting heat transfer analysis.

6.2 Material Properties

The main material properties that affect the temperature distribution within section of the steel are density, thermal conductivity, and specific heat. Thermal conductivity and specific heat are two of the main temperature-dependent thermal properties of steel. Thermal conductivity is the rate at which temperature is being transferred within the section, and specific heat is the amount of energy that is required to increase the temperature of one gram of material. Eurocode 3–2005 provides the behavior of thermal conductivity and specific heat of carbon steel as a function of time which are illustrated in Fig. 7 [45].

As illustrated in the above figures, temperature rises decrease the thermal conductivity of steel and it has almost a linear pattern. Within the temperature range of 700–800 °C, the specific heat of steel experiences a sudden jump that is caused by the phase change that steel experiences at 750 °C. The tower is made of St42 carbon steel with minimum yield strength of 400 MPa. The temperature-dependent material properties of steel were defined with respect to St42 and temperature-dependent behaviors mentioned in EC3 figures (Fig. 7). The high temperatures do not have a major impact on the density and the ambient density of steel can be used in the heat transfer analysis. The utilized material properties are presented in Table 4.

Table 4 Material properties of steel for heat transfer analysis

Temperature (°C)	Material properties		
	Density (kg/m^3)	Thermal conductivity (W/mK)	Specific heat (J/kgK)
20	7850	53.33	439.80
100	7850	50.67	487.62
200	7850	47.34	529.76
300	7850	44.01	564.74
400	7850	40.68	605.88
500	7850	37.35	666.50
600	7850	34.02	752.97
700	7850	30.69	981.84
735	7850	29.52	5000.00
800	7850	27.30	803.26
900	7850	27.30	650.00
1000	7850	27.30	650.00
1100	7850	27.30	650.00
1200	7850	27.30	650.00

The final step of the FE modeling is meshing the tower geometry. The type and size of the mesh were adopted after conducting several sensitivity analyses. A total of 10,641 elements were used to model the tower. To better capture the temperature distribution, a non-uniform mesh with more elements in non-exposed surfaces was used. So, a medium-fine mesh (0.01 m) was selected for the exposed surface, while non-exposed parts had a very fine mesh (0.005 m). The software input values for heat transfer analysis are presented in Table 5, and the final meshed model is illustrated in Fig. 6.

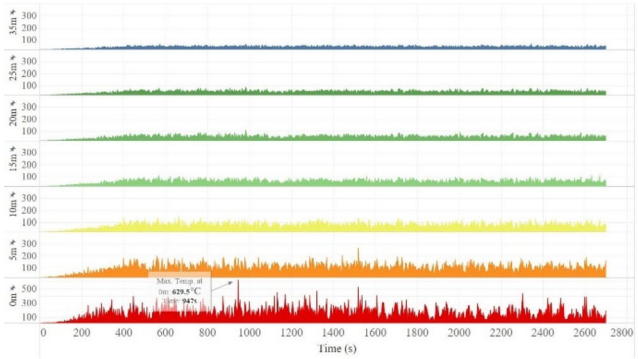

a) FS1

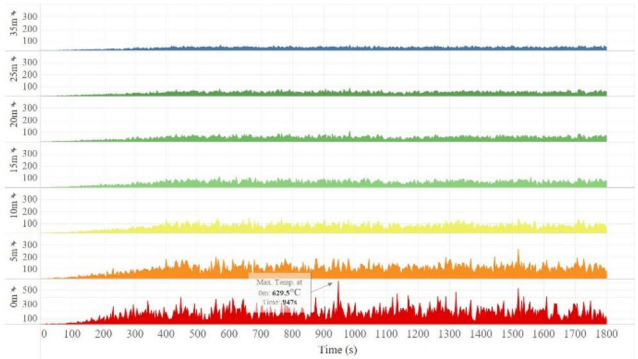

b) FS4

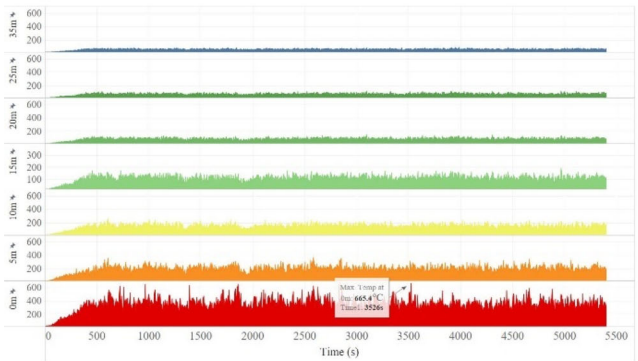

c) FS2

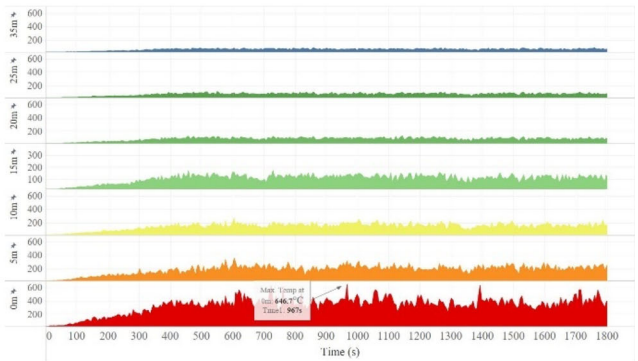

d) FS5

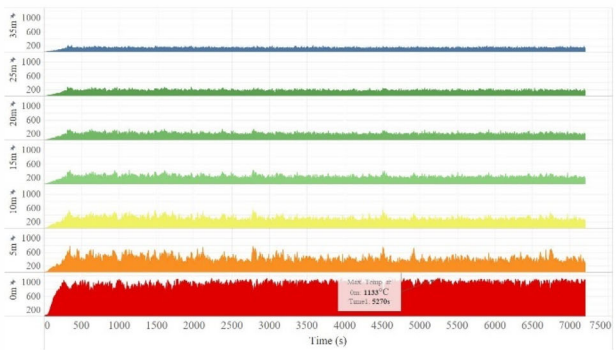

e) FS3

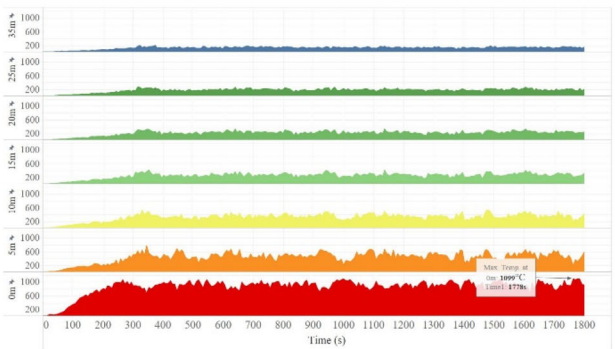

f) FS6

Fig. 5 Gas temperature developments in different scenarios

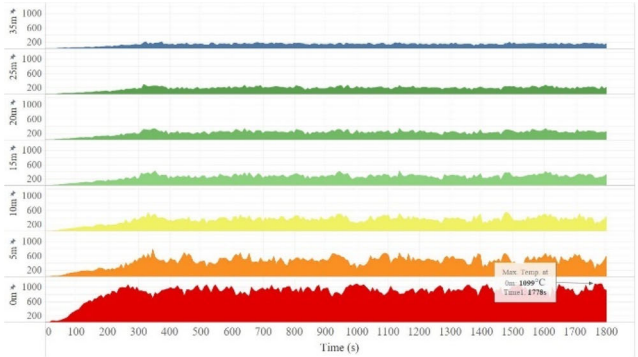

g) FS7

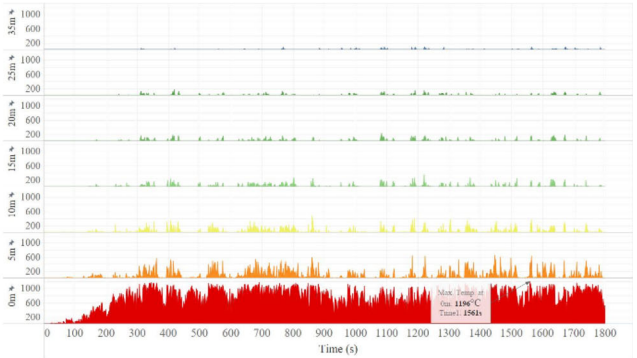

h) FS10

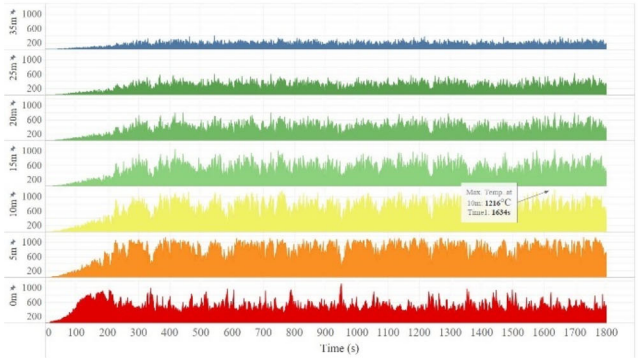

i) FS8

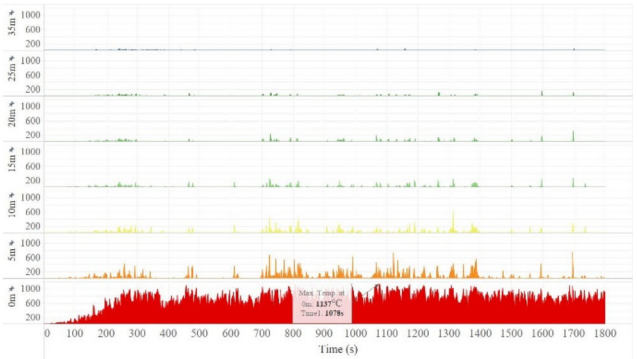

j) FS11

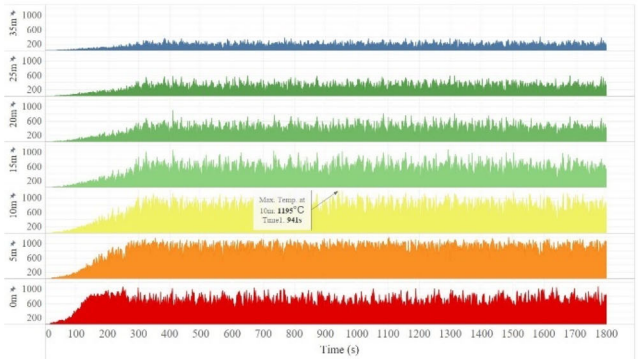

k) FS9

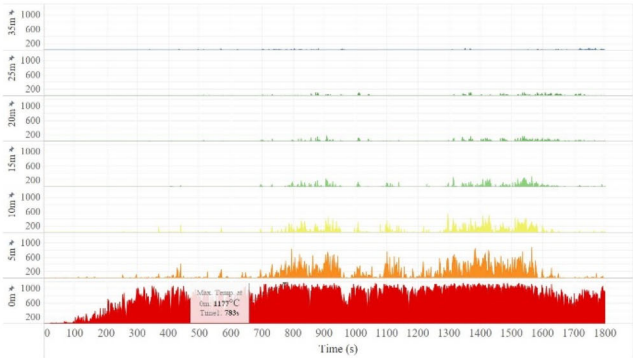

l) FS12

Fig. 5 continued

For each scenario, the AST time–temperature curves obtained from that scenario were applied as temperature loads and their time increments were adjusted accordingly. The obtained AST curves are illustrated in Fig. 8. From the results obtained from FDS, it was observed that the high temperature of the fire will not travel more than 120 m above the deck. So, the vertical fire exposure will be from 60 to 120 m of the tower.

7 Thermal Analysis Results

The temperature distributions within the tower section relevant to each scenario were obtained at different intervals of 15 min, and nodal temperature growth from some selected nodes was obtained to evaluate the effect of each fire scenario on the mechanical properties of steel. Due to a large number of results, only the nodal temperatures at the base are presented here. The location of the selected nodes, temperature development within the section, and nodal temperature growth are presented in Figs. 9, 10, and 11. Figure 12 shows

the temperature distribution within cross-section of the tower at 61 m, capturing the conditions at the completion of the burning time for each evaluated fire scenario.

8 Post-Fire Evaluations

The fire exposure to steel elements and the rapid temperature raises within the element decrease the mechanical properties of steel. After reaching the peak temperature of steel, the fire-exposed element will lose most of its strength and

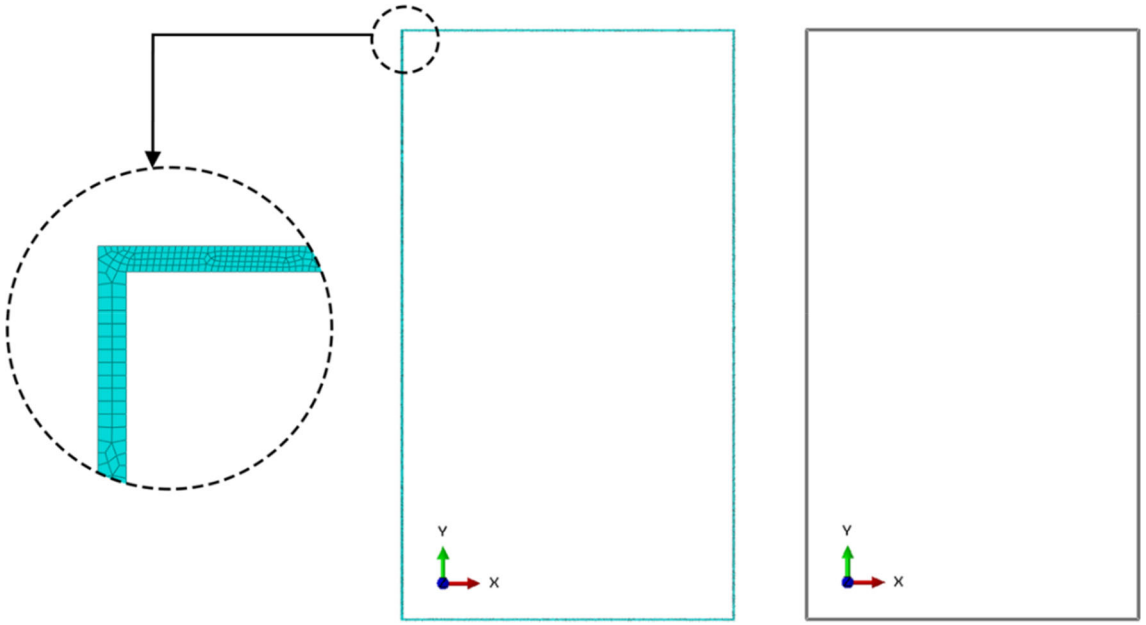

Fig. 6 FE model of the tower and the meshed element

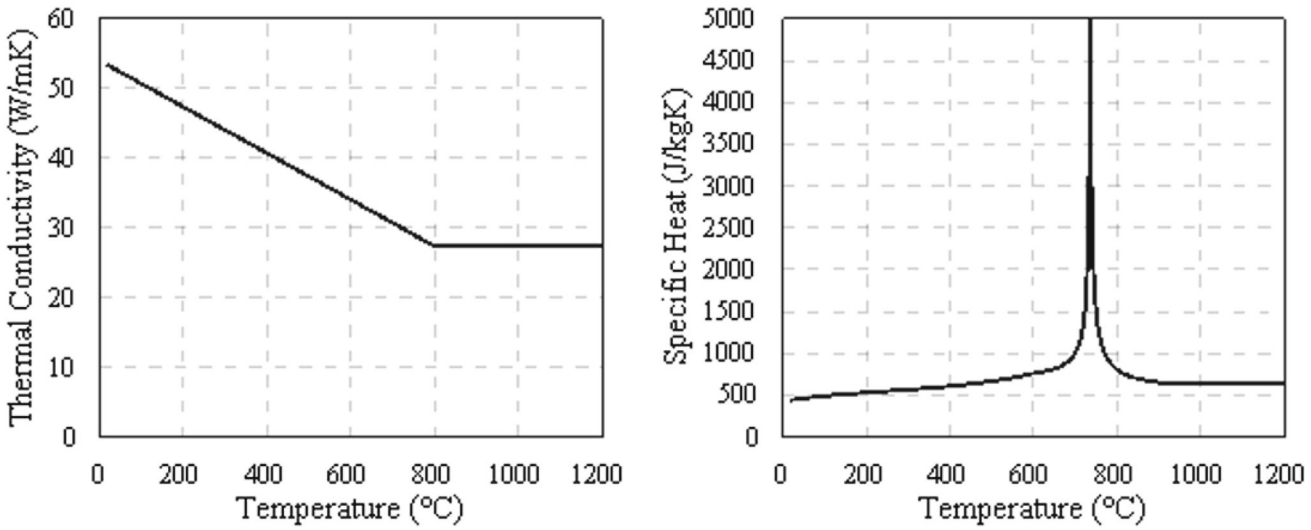

Fig. 7 Thermal properties of structural steel

Table 5 ABAQUS input values for heat transfer analysis

Element type	Approximate global mesh size (mm)	Initial temperature (°C)	Convection heat transfer coefficient (W/m^2K)	Emissivity of steel
DC2D4	1	20	50	0.7

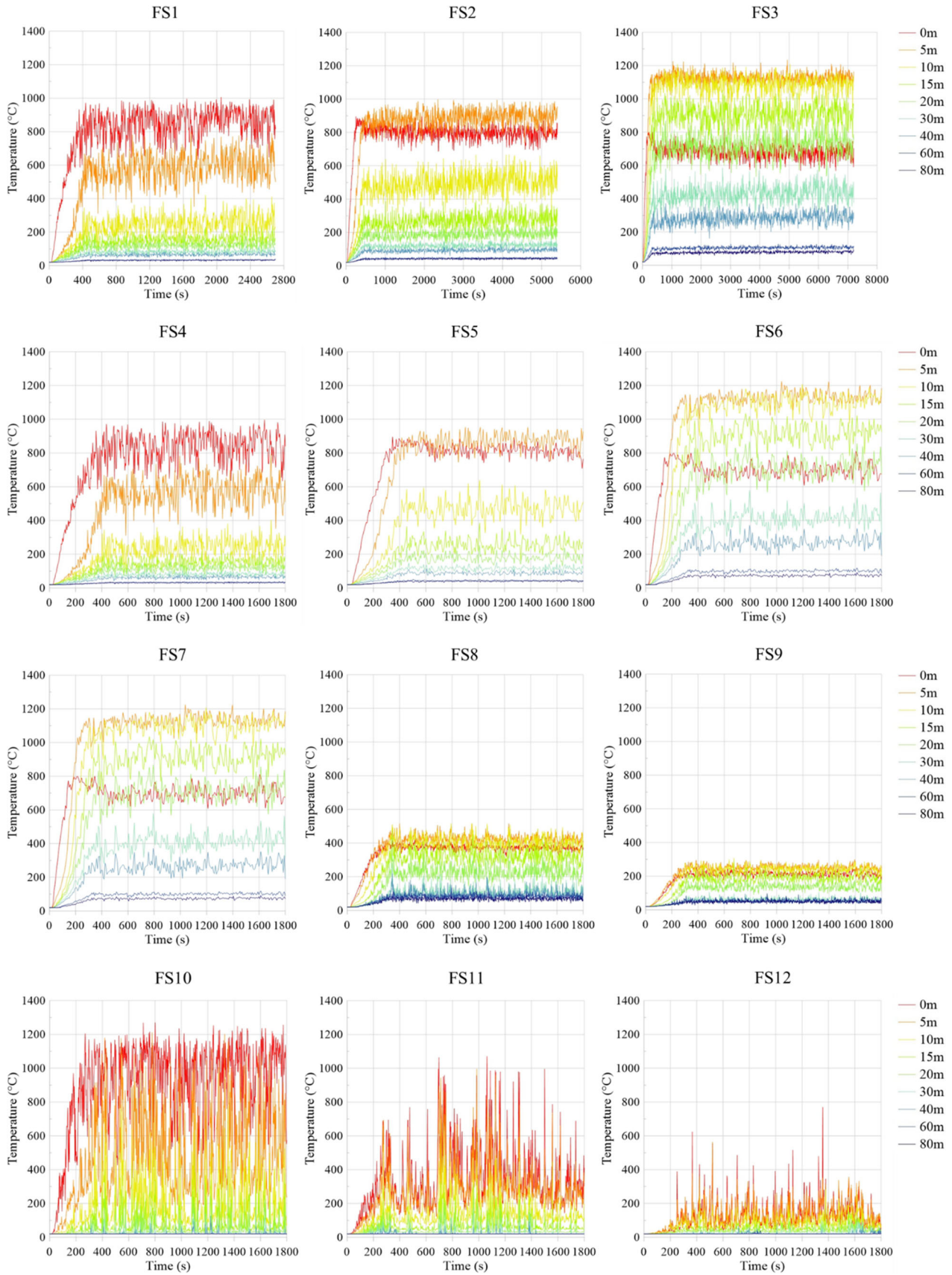

Fig. 8 AST recordings from different scenarios

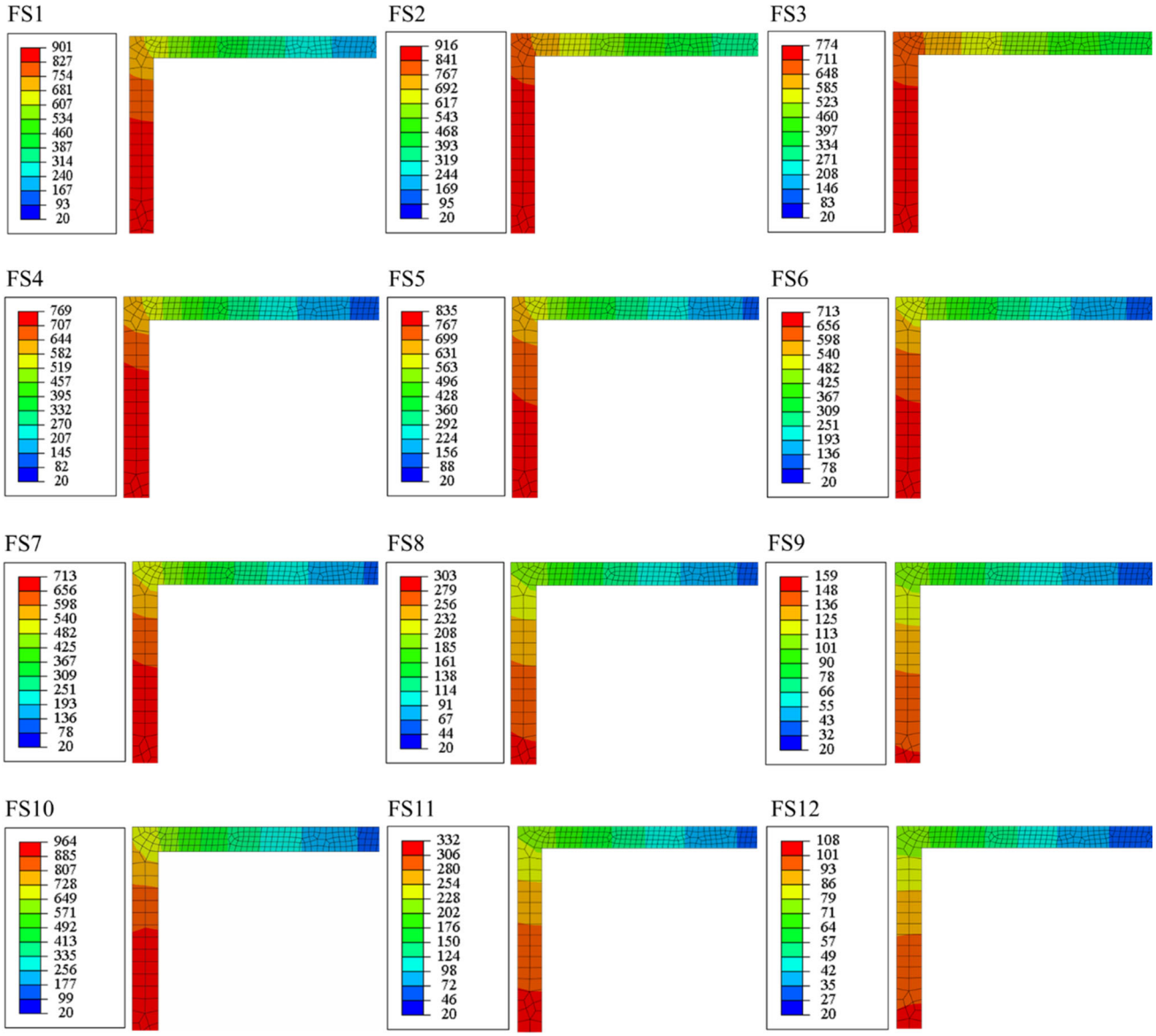

Fig. 9 Temperature distributions within section at 61 m of the tower

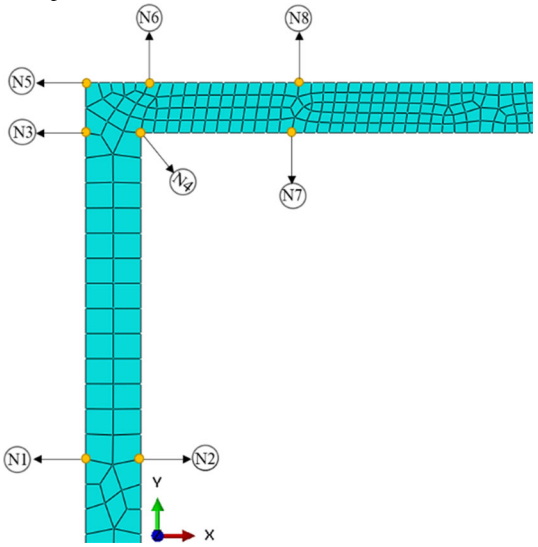

Fig. 10 Selected nodes for nodal temperature growth

bearing capacities, which results in local failures that can result in global failure of the fire-exposed structure. Generally, the fire-exposed unprotected steel member can be failed if its temperature exceeds 600 °C and when the member is not able to withstand the applied service load [46]. According to EC3, the reduction in yield strength of steel starts at 400 °C, and after exceeding 600 °C this reduction becomes more significant. The Eurocode-based temperature-dependent reduction in mechanical properties of steel is detailed in Table 6. When the steel temperature exceeds 700 °C, steel experiences a reduction of 80% in its strength and stiffness [47]. In addition, when the steel temperature exceeds 400 °C, the creep deformation becomes noticeable, and at the onset of 750 °C, the phase change occurs [45, 48]. To this end, the post-fire evaluation framework assessed the unprotected steel members based on strength loss and peak

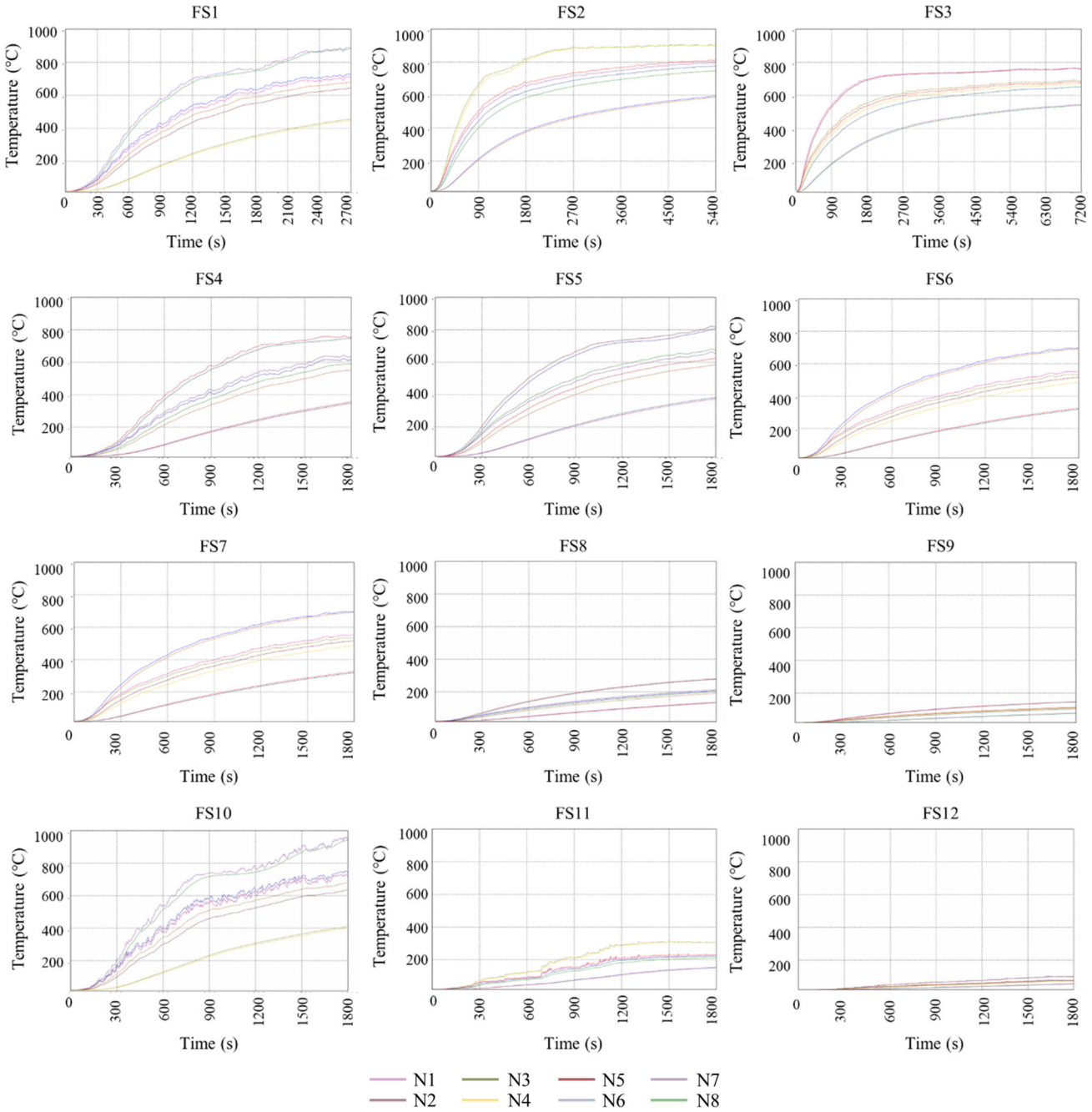

Fig. 11 Nodal temperature growth at 61 m of tower

temperatures [34, 45]. In this evaluation, damage is defined as the condition when steel temperatures exceed the critical 600 °C threshold, substantially reducing the load-bearing capacity of the member. Severe damage is identified by an 80% strength reduction, significantly undermining structural integrity. Based on the conducted 350 heat transfer analysis, the temperature developments along the tower's height were obtained, and considering reduction factors in Table 7 the strength losses for each scenario were obtained, which are presented in Fig. 13.

8.1 Vehicle Size and Exposure Duration

The results depicted in the above figures clearly demonstrate that the temperature evolution within the steel section of the tower is significantly affected by the type of vehicle involved in the fire and the duration of the burning. In the case of the fuel truck fire, which was more intense, the temperature rise within the first 15 min resulted in substantial strength loss in the lower 14 m of the tower. In contrast, the fires caused by the other two vehicle types had a minimal impact on the

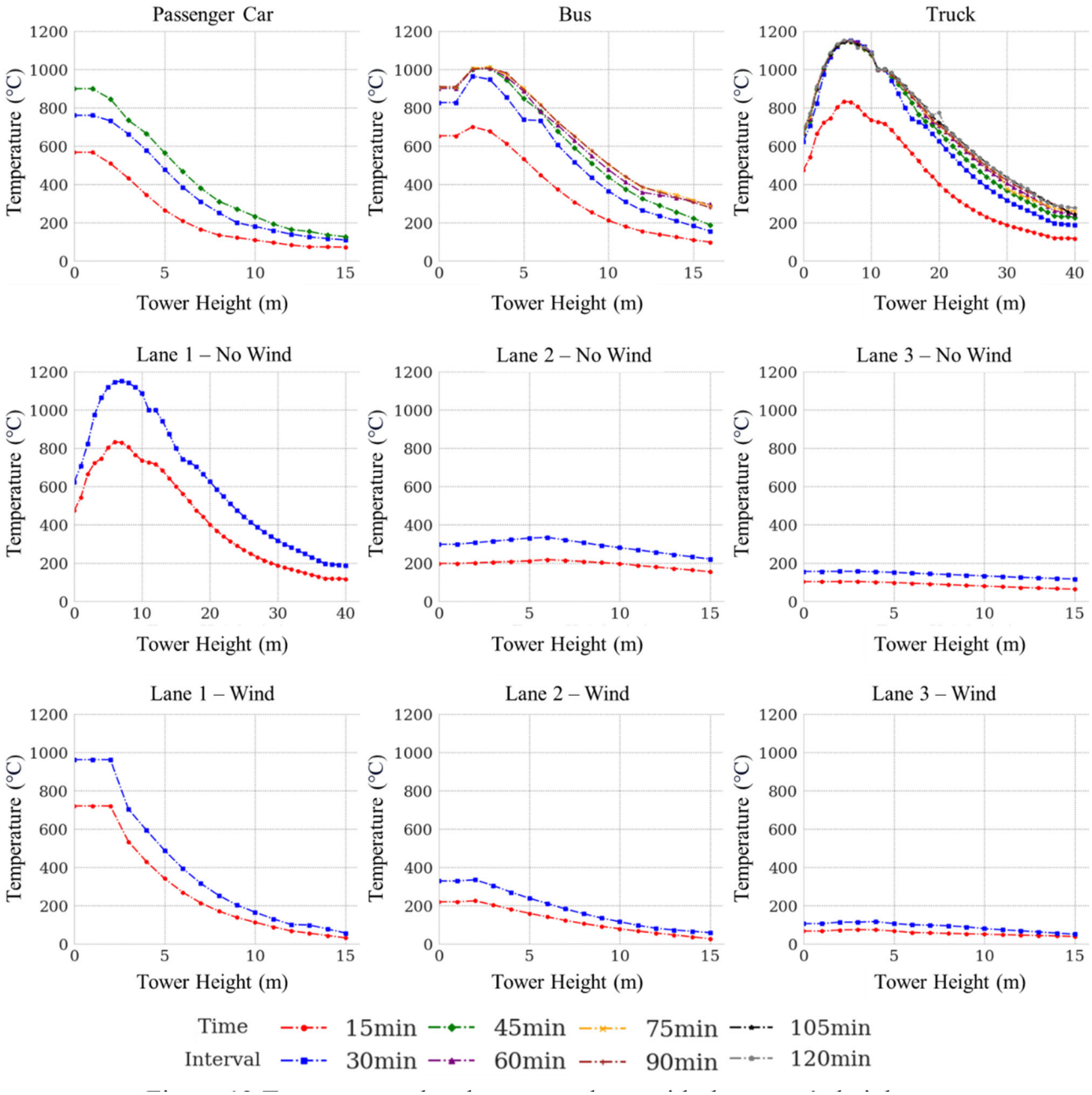

Fig. 12 Temperature developments along with the tower's height

strength of the tower. As the fuel truck fire continued for a prolonged period of 7200 s, the heat affected an even larger portion of the tower, with the first 23 m reaching temperatures indicative of the phase change zone. This would likely lead to considerable local failure in these sections of the tower, emphasizing the critical need for prompt fire suppression to mitigate the spread of damage to the higher parts of the structure. For the 5400 s of bus fire, the damage was limited to the first 8 m of the tower. In the scenario of the passenger car fire, only the very base of the tower experienced significant strength loss over the entire duration of 2700 s. These findings suggest that an unprotected steel tower has the resilience to endure the thermal impact of a passenger car fire for up to 45 min. This conclusion is based on the observed containment of strength loss exhibited in the lower regions of the tower.

8.2 Fire Distance

The distance between the burning source and the tower has major impact on the severity of fire exposure to the tower.

Table 6 Effects of temperature on mechanical properties of carbon steel

Steel temperature (°C)	Reduction factor for modulus of elasticity	Modulus of elasticity (MPa)	Reduction factor for effective yield strength	Yield strength (MPa)
20	1.000	2.05E + 11	1.00	400
100	1.000	2.05E + 11	1.00	400
200	0.900	1.85E + 11	1.00	400
300	0.800	1.48E + 11	1.00	400
400	0.700	1.03E + 11	1.00	400
500	0.600	6.20E + 10	0.78	312
600	0.310	1.92E + 10	0.47	146.64
700	0.130	2.50E + 09	0.23	33.73
800	0.090	2.25E + 08	0.11	3.71
900	0.068	1.52E + 07	0.06	0.22
1000	0.045	6.83E + 05	0.04	0.01
1100	0.023	1.54E + 04	0.02	0.00
1200	0.000	0.00E + 00	0.00	0.00

Table 7 Localized effect of different fire scenarios

Scenario	Cross-sectional temperature > 400 °C (%)	Cross-sectional temperature > 600 °C (%)	Cross-sectional temperature > 800 °C (%)	Tot. affected height (m)
FS1	17.7	< 1.0	< 1.0	6.0
FS2	18.0	17.5	< 1.0	11.0
FS3	18.3	17.8	17.3	32.0
FS4	17.7	< 1.0	< 1.0	5.0
FS5	18.1	17.5	1.0	9.0
FS6	18.3	17.6	0.0	26.0
FS7	18.3	17.6	17.3	26.0
FS8	0.0	0.0	0.0	0.0
FS9	0.0	0.0	0.0	0.0
FS10	18.1	17.6	< 1.0	4.0
FS11	0.0	0.0	0.0	0.0
FS12	0.0	0.0	0.0	0.0

The fuel truck fire on the first lane at a 1-m distance from the tower significantly increased the tower temperature, and after 30 min of exposure, the temperature of the first 20 m of the tower exceeded 600 °C and maintained an average temperature of 911 °C. But in two other scenarios, in which the burning source was on the second and third lanes, the maximum temperature of the tower was below 400 °C and tower did not experience any strength losses. So, fire from the second and third lanes cannot affect the tower.

8.3 Wind Effect

The results show that a heavy wind toward the tower intensifies the temperature load on the bottom of the tower. But it also causes a major reduction in the temperature of the higher parts. Under normal weather conditions, a 30-m fire exposure from a fuel truck on the first lane could damage the first 20 m of the tower. But under windy conditions, only 4 m of the tower had completely lost its strength, and this damage could not reach to the higher parts.

In the scenario involving a fire on the second lane, wind effects significantly influenced the thermal response of the tower. The initial 3 m of the tower exhibited a temperature increase of approximately 30 °C. Beyond this point, the rest of the tower experienced temperature decreases. After 30 min of the fire on the second lane compounded by wind effects (FS11), the temperature of the tower remained below 350 °C. Similarly, the fire load effects on the third lane (FS12)

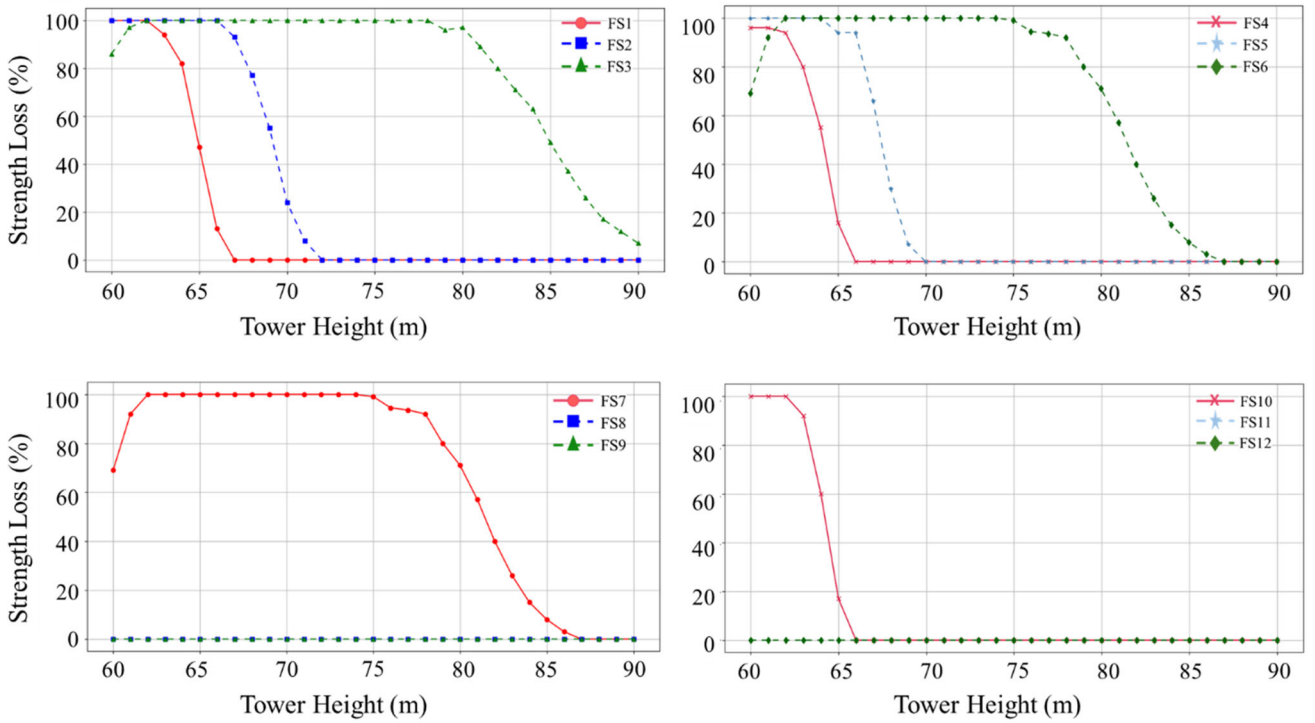

Fig. 13 Percentage of loss in strength of tower under different exposure scenarios

were mitigated by the wind, resulting in a maximum tower temperature not exceeding 150 °C. Consequently, the fires originating from the second and third lanes did not possess the severity required to induce significant strength loss or damage to the tower. Based on nodal temperature, the localized effect of the fire under each scenario is presented in Table 6. This table outlines the percentages of the tower's cross-section exceeding temperatures of 400 °C, 600 °C, and 800 °C across all scenarios.

After performing ABAQUS thermal analysis and obtaining strength losses, Cross Section Analysis & Design software was employed to evaluate the capacity of tower's section under different conditions. This evaluation particularly focused on scenarios representing the least and most severe fire conditions to illustrate the range of potential impacts on structural capacity of the tower. Initially, the tower was analyzed under its own self-weight and typical vehicle loads, representing normal operating conditions. In this state, the tower operates well within its safety margins, utilizing only about 10% (24 MPa out of 275 MPa) of its capacity. Exposure to a passenger car fire resulted in an increase in stress to 35% of the tower's capacity, a level that still falls within acceptable safety margins. However, following a 7200-s truck fire, the section has reached 60% of its total capacity, marking a significant increase. While the cross-sectional capacity decreases, the internal forces remain safely within the capacity curve, ensuring the tower can still carry loads safely. Yet, this situation increases the risk of failure. The obtained results are demonstrated in Figs. 14 and 15. The capacity of the section remained within acceptable limits under no fire and passenger car fire scenarios. In contrast, the truck fire scenario resulted in a notable reduction in capacity. Notably, this analysis did not incorporate additional temperature-dependent factors, such as thermal elongation, which suggests that the evaluated impact of the fire might represent a conservative estimate. This result highlights the critical impact of severe fire conditions on the structural integrity of steel towers, emphasizing the need for early fire detection and suppression strategies to mitigate potential damages.

An overview of the conducted bridge fire evaluation, along with the primary outcomes categorized by risk rating, is presented in Fig. 16.

9 Conclusions

This paper has evaluated the effect of fire exposure to the steel tower of suspension bridges and examined the effects of fire size, distance, time, and wind on the post-fire condition of the tower. To perform the analysis, the Bosphorus Bridge, which is one of the iconic suspension bridges in the world, was selected. A total of 12 fire scenarios arising from the mentioned parameters were simulated, and the fire characteristics as well as the post-fire condition of the tower under each fire scenario were evaluated.

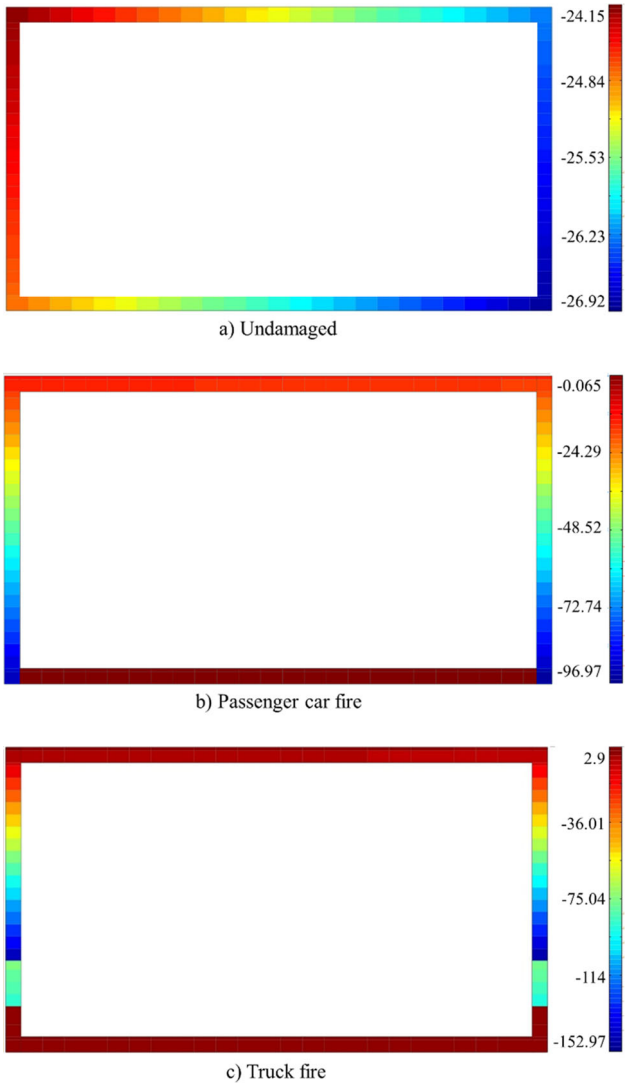

Vehicle fire with a large spill area in proximity to the tower can significantly increase the temperature of the tower and make significant reduction in its yield strength.

The front sections of the first 83 m of the tower that was engulfed by localized tanker fire had lost almost all their strength which result in severe damage.

For fires on the first lane, under normal conditions fire will spread along with the tower's height while under the windy condition the flame will only engulf the bottom parts of the tower.

Fire exposure from a vehicle on lanes 2 or 3 could not change the strength of the tower. But a fire resulting from a chain reaction vehicle accident can change the fire performance of the tower.

Due to the severity of the fuel truck fire in the vicinity of an unprotected steel tower, only 30 min of fire exposure is enough to damage 10 m of the tower and will be intensified by longer fire duration. So, early control of the fire has crucial importance in reducing the severity of the damage and preventing temperature development in higher areas of the tower.

A bus fire in the proximity of the unprotected steel tower can lead to minor damage. This can be prevented by fire strengthening the first 10 m of the tower above the deck.

The steel tower can withstand fire loads from passenger car fires and no failure would be expected.

Under normal environmental conditions, fire loads from horizontal distances more than the first lane do not put the tower at fire risk, and the unprotected steel tower can withstand the fire loads applying from the second and third lanes.

Fig. 14 Stress distribution within section of the tower

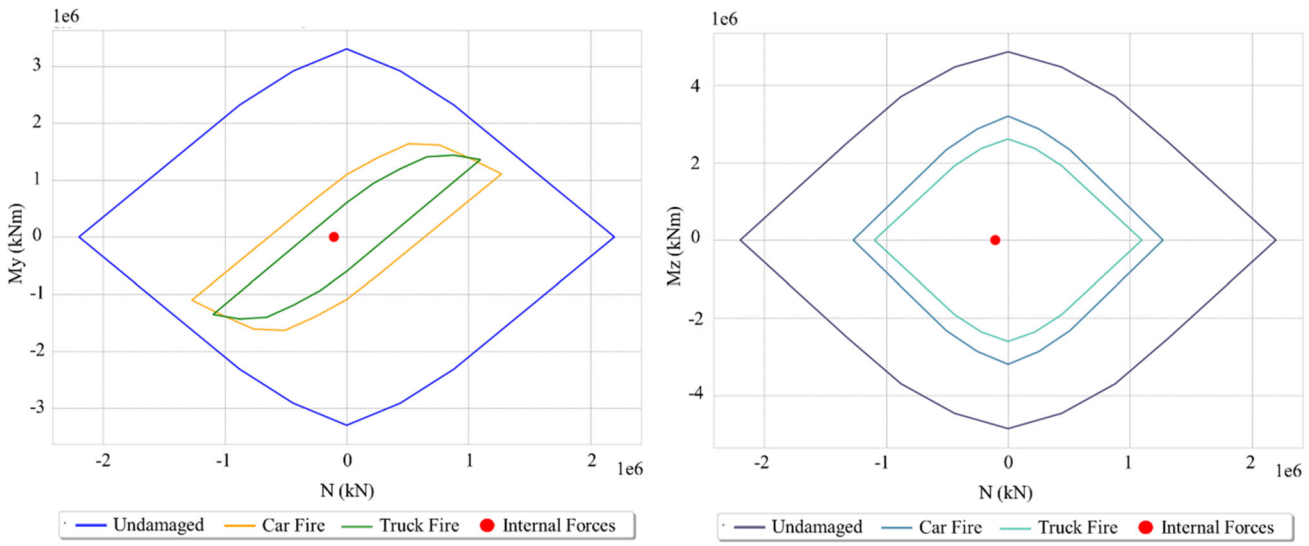

Fig. 15 Cross-sectional capacity of the tower under different conditions

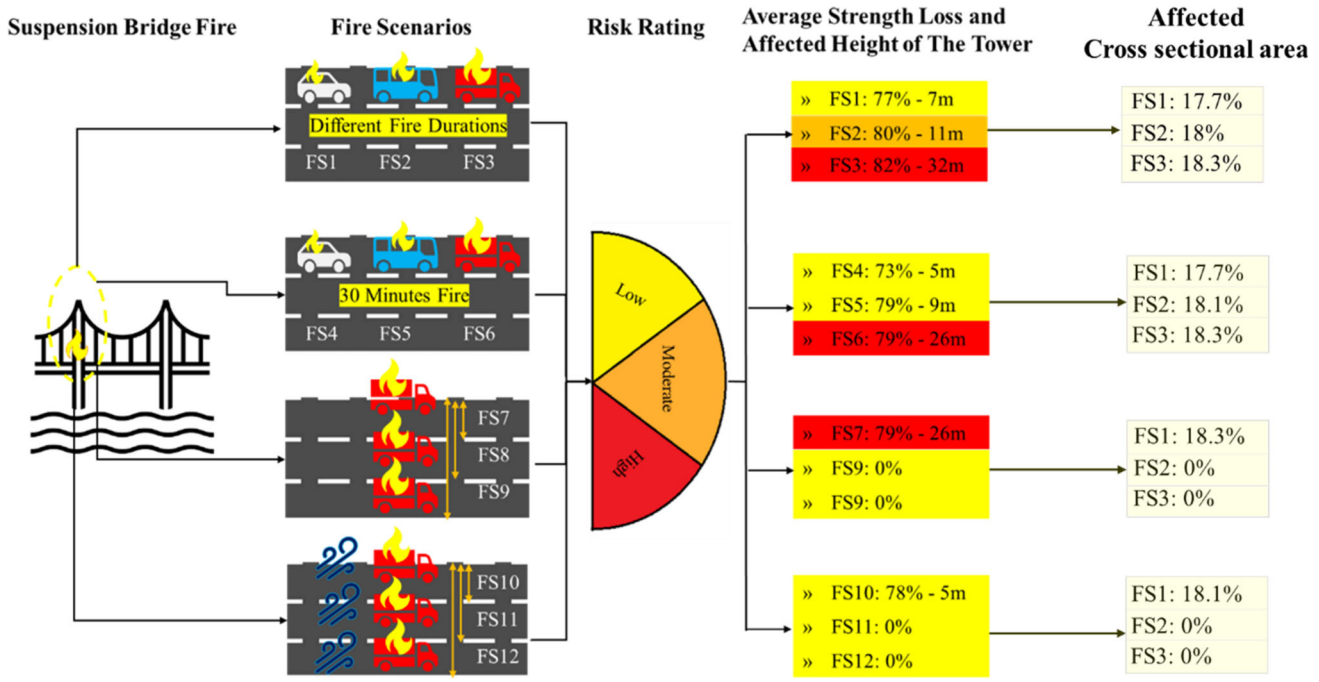

Fig. 16 Fire evaluation of the Bosphorus suspension bridge tower

A heavy wind toward the tower considerably intensifies the fire exposure to the bottom parts of the tower. But it significantly reduces the effective diameter of the fire and decreases the fire load on higher parts.

Overall, these results indicate that steel towers of suspension bridges are highly vulnerable to large vehicle fires in their vicinities. This can be intensified or lessened by a heavy wind toward the tower. The potential damage to the tower can create major structural problems for the suspension bridge. Early control of the fire has crucial importance in degree of fire damage and failure status of the tower.

This study was mainly concerned with the influential factors on the characteristics of bridge fire, and the development of a framework for evaluating the impacts of these parameters on the extent of fire damage to the tower. Further research work is required to perform structural analysis and obtain the failure types to take the required preventive measures. In addition, fire exposure from multi-vehicle accidents and under different wind conditions can result in different fire performances.

Funding Open access funding provided by the Scientific and Technological Research Council of Türkiye (TÜBİTAK).

Open Access This article is licensed under a Creative Commons Attribution 4.0 International License, which permits use, sharing, adaptation, distribution and reproduction in any medium or format, as long as you give appropriate credit to the original author(s) and the source, provide a link to the Creative Commons licence, and indicate if changes were made. The images or other third party material in this article are included in the article's Creative Commons licence, unless indicated otherwise in a credit line to the material. If material is not included in the article's Creative Commons licence and your intended use is not permitted by statutory regulation or exceeds the permitted use, you will need to obtain permission directly from the copyright holder. To view a copy of this licence, visit http://creativecommons.org/licenses/by/4.0/.

References

1. Mitoulis, S.A.; Domaneschi, M.; Cimellaro, G.P.; Casas, J.R.: Bridge and transport network resilience—a perspective. Proc. Inst. Civ. Eng. Bridge Eng. **175**(3), 138–149 (2021)
2. Zhang, G.; Zhao, X.; Lu, Z.; Song, C.; Li, X.; Tang, C.: Review and discussion on fire behavior of bridge girders. J. Traffic Transp. Eng. **9**, 422–446 (2022)
3. Liu, X.; Yu, C.; Quan, W.; Chen, L.: Inspection, materials testing and field testing of a prestressed concrete box bridge after fire exposure. Fire Saf. J.Saf. J. **108**, 102852 (2019)
4. Beneberu, E.; Yazdani, N.: Residual strength of CFRP strengthened prestressed concrete bridge girders after hydrocarbon fire exposure. Eng. Struct.Struct. **184**, 1–14 (2019)
5. Garlock, M.; Paya-Zaforteza, I.; Kodur, V.; Gu, L.: Fire hazard in bridges: review, assessment and repair strategies. Eng. Struct.Struct. **35**, 89–98 (2012)
6. Peris-Sayol, G.; Paya-Zaforteza, I.; Balasch-Parisi, S.; Alós-Moya, J.: Detailed analysis of the causes of bridge fires and their associated damage levels. J. Perform. Constr. Facil.Facil. **31**(3), 04016108 (2017)
7. Bajwa, C.S.; Easton, E.P.; Adkins, H.; Cuta, J.; Klymyshyn, N.; Suffield, S.: The Macarthur Maze fire and roadway collapse: a

"worst case scenario" for spent nuclear fuel transportation. In: Proceedings of the ASME 2012 Pressure Vessels & Piping Division Conference, (2012) PVP2012–78637
8. Quiel, S.E.; Yokoyama, T.; Bregman, L.S.; Mueller, K.A.; Marjanishvili, S.M.: A streamlined framework for calculating the response of steel-supported bridges to open-air tanker truck fires. Fire Saf. J.Saf. J. **73**, 63–75 (2015)
9. Astaneh-Asl, A.; Noble, C.R.; Son, J.; Wemhoff, A.P.; Thomas, M.P.; McMichael, L.D.: Fire protection of steel bridges and the case of the macarthur maze fire collapse, TCLEE 2009: Lifeline Earthquake Engineering in a Multihazard Environment. 357 (2009) 1–12.
10. Alos-Moya, J.; Paya-Zaforteza, I.; Garlock, M.E.M.; Loma-Ossorio, E.; Schiffner, D.; Hospitaler, A.: Analysis of a bridge failure due to fire using computational fluid dynamics and finite element models. Eng. Struct.Struct. **68**, 96–110 (2014)
11. Kodur, V.K.; Aziz, E.M.; Naser, M.Z.: Strategies for enhancing fire performance of steel bridges. Eng. Struct.Struct. **131**, 446–458 (2017)
12. Khan, M.A.; Khan, A.A.; Domada, R.; Usmani, A.: Fire hazard assessment, performance evaluation, and fire resistance enhancement of bridges. Structures. **34**, 4704–4714 (2021)
13. Kodur, V.K.R.; Naser, M.Z.: Importance factor for design of bridges against fire hazard. Eng. Struct. Struct. **54**, 207–220 (2013)
14. Hu, J.; Carvel, R.; Usmani, A.: Bridge fires in the 21st century: A literature review. Fire Saf J. **126**, 103487 (2021)
15. Akbulut, Y.E.; Altunişik, A.C.; Başağa, H.B.; Mostofi, S.; Mosallam, A.; Wafa, L.F.: Elevated temperature effect on the dynamic characteristics of steel columns and frames. Int. J. Steel Struct. **21**, 861–882 (2021)
16. Naser, M.Z.; Kodur, V.K.R.: Comparative fire behavior of composite girders under flexural and shear loading. Thin-Walled Struct. pp 82–90 (2017)
17. Naser, M.; Kodur, V.: Response of fire exposed composite girders under dominant flexural and shear loading. J. Struct. Fire Eng. **9**, 108–125 (2018)
18. Kodur, V.K.R.; Naser, M.Z.: Designing steel bridges for fire safety J. Construct. Steel Res. **156**, 46–53 (2019). https://doi.org/10.1016/j.jcsr.2019.01.020
19. The National Fire Protection Association (NFPA): Free Access - NFPA 502: Standard for Road Tunnels, Bridges, and Other Limited Access Highways. (2023)
20. Paya-Zaforteza, I.; Peris-Sayol, G.: Bridge Fires: Fiction or Reality? - SFPE. https://www.sfpe.org/publications/periodicals/sfpeeuropedigital/sfpeeurope6/issue6feature3
21. Xi-qiang, W.; Ting, H.F.T.K.; Au Jing, L.: Posttensioned concrete bridge beams exposed to hydrocarbon fire. J. Struct. Eng. (2020). https://doi.org/10.1061/(ASCE)ST.1943-541X.0002791
22. Song, C.; Zhang, G.; Li, X.; Kodur, V.: Experimental and numerical study on failure mechanism of steel-concrete composite bridge girders under fuel fire exposure. Eng. Struct. **247**, 113230 (2021). https://doi.org/10.1016/j.engstruct.2021.113230
23. Zhang, Z.; Guo, T.; Wang, S.; Liu, J.; Wang, L.: Experimental study on post-fire properties of steel wires of bridge suspender. Structures **33**, 1252–1262 (2021). https://doi.org/10.1016/j.istruc.2021.04.099
24. Eyosias, B.; Nur, Y.: Performance of CFRP-strengthened concrete bridge girders under combined live load and hydrocarbon fire. J. Bridge Eng. (2018). https://doi.org/10.1061/(ASCE)BE.1943-5592.0001244
25. Alos-Moya, J.; Paya-Zaforteza, I.; Hospitaler, A.; Rinaudo, P.: Valencia bridge fire tests: Experimental study of a composite bridge under fire. J Construct. Steel Res. **138**, 538–554 (2017). https://doi.org/10.1016/j.jcsr.2017.08.008
26. Vimonsatit, V.; Tan, K.H.; Qian, Z.H.: Testing of Plate Girder Web Panel Loaded in Shear at Elevated Temperature. J. Struct. Eng. **133**(6), 815–824 (2007). https://doi.org/10.1061/(ASCE)0733-9445(2007)133:6(815)
27. Aziz, E.M.; Kodur, V.K.; Glassman, J.D.; Moreyra Garlock, M.E.: Behavior of steel bridge girders under fire conditions. J. Construct. Steel Res. **106**, 11–22 (2015). https://doi.org/10.1016/j.jcsr.2014.12.001
28. Chen, C.; Chen, J.; Zhao, X.; Shi, C.: Experimental investigation on combustion characteristics of steel cable for cable-stayed bridge. J Therm Anal Calorim. **134**, 2317–2327 (2018). https://doi.org/10.1007/S10973-018-7689-6/FIGURES/16
29. Bennetts, I.; Moinuddin, K.: Evaluation of the impact of potential fire scenarios on structural elements of a cable-stayed bridge. J. Fire Protection Eng. **19**(2), 85–106 (2009). https://doi.org/10.1177/1042391508095091
30. Payá-Zaforteza, I.; Garlock, M.E.M.: A numerical investigation on the fire response of a steel girder bridge. J. Construct. Steel Res. **75**, 93–103 (2012). https://doi.org/10.1016/j.jcsr.2012.03.012
31. Xu, G.; Agrawal A.K.: Safety of Cable-Supported Bridges during Fire Hazards. J. Bridge Eng. (2016). https://doi.org/10.1061/(ASCE)BE.1943-5592.0000870
32. Peris-Sayol G.; Paya-Zaforteza, I.; Alos-Moya, J.; Hospitaler, A.: Analysis of the influence of geometric modeling and environmental parameters on the fire response of steel bridges subjected to realistic fire scenarios. Comput. Struct. **158**, 333–345 (2015). https://doi.org/10.1016/j.compstruc.2015.06.003
33. Alos-Moya, J.; Paya-Zaforteza, I.; Hospitaler, A.; Loma-Ossorio, E.: Valencia bridge fire tests: Validation of simplified and advanced numerical approaches to model bridge fire scenarios. Adv. Eng. Software **128**, 55–68 (2019). https://doi.org/10.1016/j.advengsoft.2018.11.003
34. Cui, C.; Chen, A.; Ma, R.: Stability assessment of a suspension bridge considering the tanker fire nearby steel-pylon. J. Const. Steel Res. (2020). https://doi.org/10.1016/j.jcsr.2020.106186
35. Zou, Q.; Pool, K.; Chen, S.: Performance of suspension bridge hangers exposed to hazardous material fires considering wind effects. **9**, 1–16 (2020)
36. Chen, W.-F.; Duan, L.: Bridge Engineering Handbook, 2nd edn. CRC Press, Taylor & Francis group, Boca Raton, Florida, USA (2014)
37. ABAQUS. Dassault Systèmes. Simulia Corporation (2016)
38. Thunderhead Engineering. (2022). PyroSim
39. Ma, R.; Cui, C.; Ma, M.; Chen, A.: Performance-based design of bridge structures under vehicle-induced fire accidents: Basic framework and a case study. Eng. Struct. (2019). https://doi.org/10.1016/j.engstruct.2019.109390
40. Aslan, H.; Kuyuk, H.S.; Aktas, M.: Transportation risk analysis (TRA) of bosphorus suspended bridge, using probabilistic approach. Vulnerability, Uncertainty, and Risk: Analysis, Modeling, and Management - Proceedings of the ICVRAM 2011 and ISUMA 2011 Conferences. pp 683–690 (2011)
41. Adanur, S.; Okur, E.K.; Altunişik, A.C.; Günaydin, M.; Rahwan, B.R.: Investigation of the structural behaviors of Bosphorus suspension bridge with vertical hangers replaced by inclined hangers. Alexandria Eng. J. **65**, 75–102 (2023). https://doi.org/10.1016/j.aej.2022.10.041
42. McGrattan, K.; Hostikka, S.; McDermott, R.; Floyd, J.; Weinschenk, C.; Overhold, K.: Fire Dynamics Simulator Technical Reference Guide Volume 2: Verification. National Insitute of Standards and Technology. **1**, 201 (2019)
43. Janssens, M.L.: Handbook of Environmental Degradation of Materials. William Andrew Publishing (2018)
44. Hurley, M.J.; Gottuk, D.T.; Hall Jr, J.R.; Harada, K.; Kuligowski, E.D.; Puchovsky, M.; Watts Jr, J.M.; Wieczorek, C.J: SFPE Handbook of Fire Protection Engineering, Fifth Edition. (2016)
45. EN 1993-1-2: Eurocode 3: Design of steel structures - Part 1-2: General rules - Structural fire design. (1993)

46. Wright, W.; Lattimer, B.; Woodworth, M.; Nahid, M.; Sotelino, E.: Highway Bridge Fire Hazard Assessment. (2013)
47. Li Guoqiang, P.W.: Advanced Analysis and Design for Fire Safety of Steel Structures. ZHEJIANG UNIVERSITY PRESS (2012)
48. Venkatesh, K.; Mahmud, D.; Rustin, F.: High-Temperature properties of steel for fire resistance modeling of structures. J. Mater. Civil Eng. **22**, 423–434 (2010). https://doi.org/10.1061/(ASCE)MT.1943-5533.0000041
49. Süleyman, A.; Ahmet, C.; Altunişik, A.; Bayraktar Mehmet, A.: Comparison of near-fault and far-fault ground motion effects on geometrically nonlinear earthquake behavior of suspension bridges. Nat. Hazards **64**(1), 593–614 (2012). https://doi.org/10.1007/s11069-012-0259-5
50. Günaydin, M.; Adanur, S.; Can Altunişik, A.; Sevim, B.; Adanur, S.; Sevım, B.; Türker, E.: Determination of structural behavior of Bosporus suspension bridge considering construction stages and different soil conditions. Steel Composite Struct. **17**, 405–429 (2014)